MR Imaging Relaxation Times of Abdominal and Pelvic Tissues Measured in Vivo at 3.0 T: Preliminary Results

Cedric M. J. de Bazelaire, MD
Guillaume D. Duhamel, PhD
Neil M. Rofsky, MD
David C. Alsop, PhD

Index terms:
Abdomen, MR, 761.12146, 770.12146, 775.12146
Magnetic resonance (MR), tissue characterization
Pelvis, MR, 844.12146, 854.12146

Published online
10.1148/radiol.2303021331
Radiology 2004; 230:652–659

Abbreviations:
ROI = region of interest
SE = spin echo
TE = echo time
TI = inversion time
TR = repetition time

[1] From the Department of Radiology, Center for Advanced Imaging/West, CC090, Beth Israel Deaconess Medical Center, 1 Deaconess Rd, Boston, MA 02215. Received October 16, 2002; revision requested December 23; final revision received May 22, 2003; accepted July 1. Supported in part by the French Society of Radiology (SFR), the French Association for Research in Oncology (ARC), and the National Institute of Biomedical Imaging and Bioengineering grant R21EB00562. **Address correspondence to** C.M.J.d.B. (e-mail: *cdebazel@caregroup.harvard.edu*).

Author contributions:
Guarantor of integrity of entire study, C.M.J.d.B.; study concepts, C.M.J.d.B., D.C.A., N.M.R.; study design, C.M.J.d.B., D.C.A.; literature research, C.M.J.d.B., D.C.A.; clinical and experimental studies, C.M.J.d.B.; data acquisition, C.M.J.d.B., D.C.A., G.D.D.; data analysis/interpretation, C.M.J.d.B.; statistical analysis, C.M.J.d.B.; manuscript preparation, C.M.J.d.B.; manuscript definition of intellectual content, all authors; manuscript editing, C.M.J.d.B.; manuscript revision/review, D.C.A., N.M.R.; manuscript final version approval, all authors

MR Imaging Relaxation Times of Abdominal and Pelvic Tissues Measured in Vivo at 3.0 T: Preliminary Results[1]

PURPOSE: To measure T1 and T2 relaxation times of normal human abdominal and pelvic tissues and lumbar vertebral bone marrow at 3.0 T.

MATERIALS AND METHODS: Relaxation time was measured in six healthy volunteers with an inversion-recovery method and different inversion times and a multiple spin-echo (SE) technique with different echo times to measure T1 and T2, respectively. Six images were acquired during one breath hold with a half-Fourier acquisition single-shot fast SE sequence. Signal intensities in regions of interest were fit to theoretical curves. Measurements were performed at 1.5 and 3.0 T. Relaxation times at 1.5 T were compared with those reported in the literature by using a one-sample *t* test. Differences in mean relaxation time between 1.5 and 3.0 T were analyzed with a two-sample paired *t* test.

RESULTS: Relaxation times (mean ± SD) at 3.0 T are reported for kidney cortex (T1, 1,142 msec ± 154; T2, 76 msec ± 7), kidney medulla (T1, 1,545 msec ± 142; T2, 81 msec ± 8), liver (T1, 809 msec ± 71; T2, 34 msec ± 4), spleen (T1, 1,328 msec ± 31; T2, 61 msec ± 9), pancreas (T1, 725 msec ± 71; T2, 43 msec ± 7), paravertebral muscle (T1, 898 msec ± 33; T2, 29 msec ± 4), bone marrow in L4 vertebra (T1, 586 msec ± 73; T2, 49 msec ± 4), subcutaneous fat (T1, 382 msec ± 13; T2, 68 msec ± 4), prostate (T1, 1,597 msec ± 42; T2, 74 msec ± 9), myometrium (T1, 1,514 msec ± 156; T2, 79 msec ± 10), endometrium (T1, 1,453 msec ± 123; T2, 59 msec ± 1), and cervix (T1, 1,616 msec ± 61; T2, 83 msec ± 7). On average, T1 relaxation times were 21% longer ($P < .05$) for kidney cortex, liver, and spleen and T2 relaxation times were 8% shorter ($P < .05$) for liver, spleen, and fat at 3.0 T; however, the fractional change in T1 and T2 relaxation times varied greatly with the organ. At 1.5 T, no significant differences ($P > .05$) in T1 relaxation time between the results of this study and the results of other studies for liver, kidney, spleen, and muscle tissue were found.

CONCLUSION: T1 relaxation times are generally higher and T2 relaxation times are generally lower at 3.0 T than at 1.5 T, but the magnitude of change varies greatly in different tissues.

In pursuit of a higher signal-to-noise ratio, faster imaging, and new forms of contrast enhancement, the imaging community has been installing an increasing number of magnetic resonance (MR) imagers that operate with field strengths of 3.0 T and higher. Initially motivated by specialized research applications such as functional neuroimaging, many of these MR imagers are now being equipped with body transmit coils and surface coil arrays that enable the development of body imaging applications.

Optimization of body imaging protocols at 3.0 T requires an appreciation of the changes in T1 and T2 relaxation times, which accompany the change in field strength. These relaxation times help determine the contrast in MR images, and they can also affect both the spatial resolution and the signal-to-noise ratio. Furthermore, relaxation times directly affect the selection of image pulse sequence timing parameters, which affect the total

imaging times and, consequently, patient throughput (1). T1 and T2 are known to change substantially with field strength, but the change is determined with water mobility and other tissue properties in such a way that it cannot be predicted accurately with a theoretical calculation. Thus, the accurate determination of proton relaxation times with high-field-strength MR imaging is an essential first step in exploring the capabilities of high-field-strength MR imagers. While such values have been reported for the brain (2), to our knowledge values for body tissues are not currently available.

A large number of techniques for measuring T1 and T2 relaxation times in tissues have been reported (3). These methods, however, often require very long imaging times, which makes them susceptible to imaging artifacts caused by patient motion. Thus, relaxation parameters in the human abdomen have been determined only rarely. The purpose of our study was to measure T1 and T2 relaxation times of normal human abdominal and pelvic tissues and lumbar vertebral bone marrow at 3.0 T.

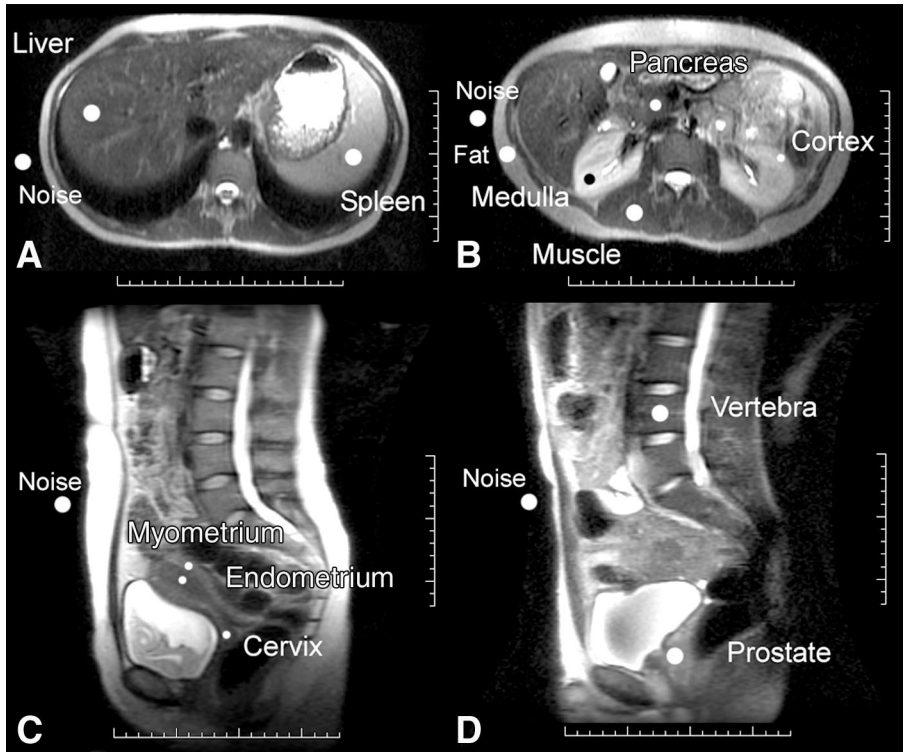

Figure 1. MR images obtained at 3.0 T with a half-Fourier acquisition single-shot fast SE sequence combined with inversion recovery (repetition time [TR], 5,000 msec; inversion time [TI], 150 msec; field of view, 360 × 252 mm; section thickness, 5 mm; acquisition matrix, 256 × 160; effective TE, 60 msec). Transverse sections through *A*, the liver and the spleen and *B*, the level of the kidney. Sagittal sections through *C*, the uterus, and *D*, the prostate and vertebra were used to generate the regions of interest (ROIs), which are indicated by white circles and labels. The scale is in centimeters.

MATERIALS AND METHODS

Subjects

The study was conducted by following a protocol approved by the Beth Israel Deaconess Medical Center Committee on Clinical Investigations, and written informed consent was obtained from each volunteer. Six healthy adults (three men and three women) with neither history nor physical findings of disease were enrolled in the study. The mean age of men was 33 years (age range, 27–37 years), and the mean age of women was 30 years (age range, 27–32 years). On the basis of reported values for the mean and SD of T1 relaxation time at 1.5 T (4) and theoretical predictions from another work (3), the size of this study permits the demonstration of differences in T1 relaxation time at 1.5 and 3.0 T in liver, spleen, and muscle tissue, with a significance and a power of 95%.

MR Imaging

All volunteers underwent imaging with a whole-body 3.0-T MR imager (VH/i; GE Medical Systems, Milwaukee, Wis) equipped with a body transmit coil. MR imaging was performed with a receive-only surface coil array (Gore Electronics, Newark, Del) that was optimized for imaging the abdomen and the pelvis. Four of the six volunteers (two men and two women) also underwent imaging with a whole-body 1.5-T MR imager (Twinspeed; GE Medical Systems) with similar coil configuration and pulse sequences for validation and comparison of the results. Two of the six volunteers were not available to undergo 1.5-T MR imaging. Images were acquired as single sections to avoid intersection modulation effects. A matrix of 256 × 160 pixels was used, with a field of view of 360 × 252 mm and a section thickness of 5 mm. A half-Fourier acquisition single-shot fast spin-echo (SE) sequence with an effective echo time (TE) of 60 msec was used to acquire each image in less than 1 second. Two transverse sections of the upper abdomen and one sagittal section of the pelvis were obtained. One of the transverse sections was positioned at the dome of the liver and the spleen, and the other was positioned at a more inferior level that depicted the kidney, the pancreas in the retroperitoneal space, the subcutaneous fat, and the paravertebral muscle (Fig 1). A sagittal view was selected for the uterus, the prostate, and the bone marrow in the L4 vertebra.

Measurements

The T1 relaxation time was measured by using an inversion-recovery preparation with a variable TI applied before the single-shot fast SE imaging sequence (Fig 2, *A*). A constant TR of 5,000 msec and a TE of 60 msec were maintained. In this experiment, images were acquired with the following six TI values: 100, 150, 250, 500, 750, and 1,000 msec. A section-selective adiabatic inversion pulse was used to ensure good inversion throughout the field of view, even in the presence of variations in the amplitude of the radiofrequency field. The inversion was performed over a section thickness twice that of the imaged section thickness to avoid the imperfect inversion near the edges of the inverted section.

For measurement of T2 relaxation times, a variable preparation delay between the 90° excitation pulse and the first refocusing pulse of the single-shot fast SE imaging sequence was used to vary the SE T2 contrast of the single-shot fast SE images (5). An equal delay between the following refocusing pulses

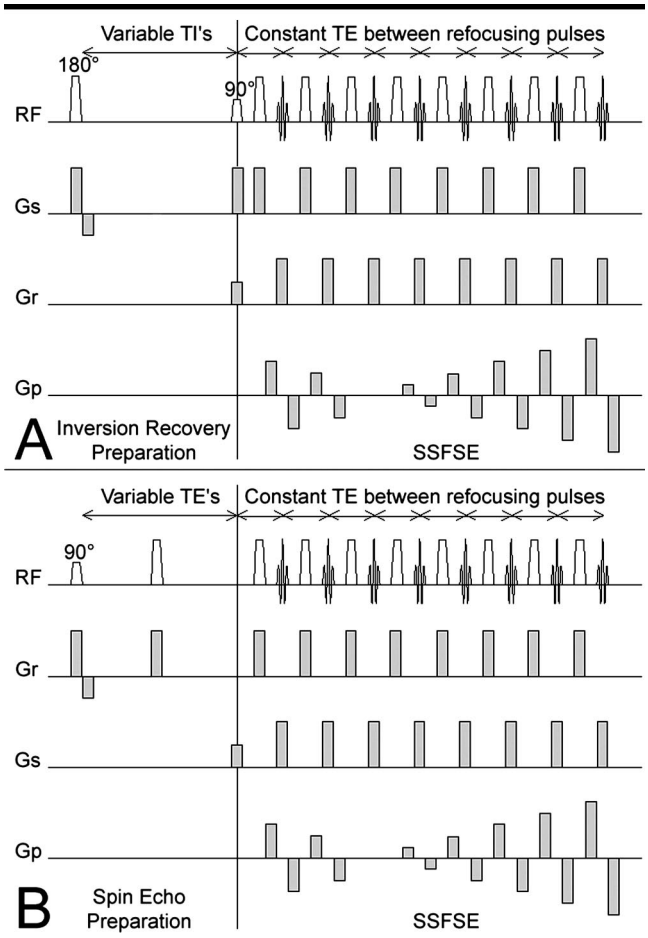

Figure 2. *A*, Diagram of the single-shot fast SE sequence (*SSFSE*) combined with multiple inversion recovery for measurement of T1 relaxation time. *B*, SE preparation for the measurement of T2 relaxation time. In *A*, the T1 contrast was obtained by using an inversion-recovery preparation with a variable TI applied before the single-shot fast SE imaging sequence. In *B*, a variable delay between the 90° excitation pulse and the first refocusing pulse of the single-shot fast SE imaging sequence was used to vary the SE T2 contrast of the single-shot fast SE images. An equal delay between the following refocusing pulses was used in the single-shot fast SE imaging sequence. The T2 contrast imparted by the phase ordering of the single-shot fast SE sequence was constant.

was used in the single-shot fast SE imaging sequence, as shown in Figure 2, *B*. A constant TR of 2,000 msec was selected. Because single-shot fast SE imaging was used for all acquisitions, this TR is the time between acquisitions of images with different TE values. Images were acquired with each of the following TE values: 15, 27, 42, 72, 122, and 202 msec. The T2 contrast imparted by the phase ordering of the single-shot fast SE sequence was constant in the images and was not included in the calculation of T2 relaxation time. Because the same refocusing pulse was used for each of the TE values, imperfections in the refocusing pulse amplitude and section profile did not affect the measurement of T2 relaxation time.

Two MR examinations were performed with all the properties of image acquisition except data collection at the beginning of the prepared single-shot fast SE sequence to achieve magnetization equilibrium so that the first TE or TI measurement would not be contaminated by magnetization saturation effects.

The single-shot fast SE sequence has considerably shorter measurement times than other standard techniques (6). The total imaging time required for measurement of T1 and T2 relaxation times was 30 and 15 seconds, respectively. Both protocols used to measure T1 and T2 were performed during a breath hold in a single session.

Validation

The prepared single-shot fast SE sequence was validated against the results obtained with a multiexcitation inversion-recovery SE sequence for the longitudinal relaxation times and a multiexcitation SE sequence for the transverse relaxation times, as described previously in the literature (6). Four averages were used with the reference sequence to improve the signal-to-noise ratio. We used eight phantoms with different concentrations of $MnCl_2$ in water. T1 and T2 relaxation times were measured at 3.0 T with the single-shot fast SE sequence by using the same parameters used for in vivo imaging. T1 relaxation times were compared with data obtained by using the multiexcitation inversion-recovery sequence with a constant TR of 5,000 msec and the following six TI values: 100, 150, 250, 500, 750, and 1,000 msec. For T2 relaxation time, the validation was made by using a multiexcitation SE sequence with a constant TR of 3,000 msec and the following six echo times: 15, 27, 42, 72, 122, and 202 msec.

Data Processing

All images were saved and transferred to a workstation (Advantage Windows 4.0; GE Medical Systems) for processing. In the following, all the ROI size values are expressed as mean number of pixels ± SD across subjects. In all subjects, the ROI was defined by the same radiologist (C.M.J.d.B.) in the liver (282 pixels ± 93), spleen (395 pixels ± 113), kidney, pancreas (68 pixels ± 27), subcutaneous fat (72 pixels ± 14), bone marrow of the L4 vertebra (105 pixels ± 31), paravertebral muscle (220 pixels ± 93), and uterus and prostate (56 pixels ± 16). Two different ROIs were drawn in the cortex (69 pixels ± 15) and the medulla (71 pixels ± 14) of the kidney. The kidney, in which the cortex was best delineated, was selected for analysis to improve ROI definition. The subcutaneous fat was selected on the transverse section in the flank at an approximately equal distance from the posterior and the anterior coils. In the uterus, the ROIs for the endometrium (30 pixels ± 21), myometrium (65 pixels ± 36), and cervix (34 pixels ± 16) were recorded as independent data points. ROIs were defined in parenchyma, and care was exercised in selecting ROIs to avoid vascular structures.

For each section location, an ROI was also defined in an empty region (200 pix-

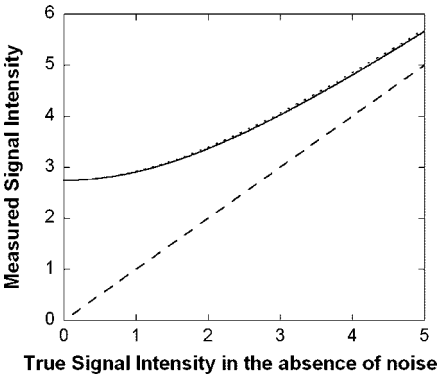

Figure 3. Simulation of the systematic error introduced by using magnitude images in the presence of noise. For a range of true signal intensities detected in one coil of a four-coil array (dashed line), the signal intensity that would be measured on a magnitude image in the presence of noise was calculated, in accordance with reference 8. A constant noise SD of 1 was assumed for each coil. This simulated magnitude signal (solid line) is much higher than the true signal intensity in the absence of noise. An approximate expression for measured signal that takes into account the noise level (Eq [1]) is also plotted as a dotted line; however, the agreement with the true curve is so good that the dotted line is mostly obscured by the solid line.

TABLE 1
Average T1 Relaxation Times at 1.5 and 3.0 T

Tissue	1.5 T		3.0 T		
	T1 Relaxation Time (msec)*	R^2 Value (%)	T1 Relaxation Time (msec)*	R^2 Value (%)	Difference (%)
Kidney					
Cortex	966 ± 58	0.999	1,142 ± 154	0.990	18†
Medulla	1,412 ± 58	0.997	1,545 ± 142	0.999	9
Liver	586 ± 39	0.995	809 ± 71	0.987	38†
Spleen	1,057 ± 42	0.998	1,328 ± 31	0.998	26†
Pancreas	584 ± 14	0.982	725 ± 71	0.976	24
Paravertebral muscle	856 ± 61	0.988	898 ± 33	0.988	5
Bone marrow (L4 vertebra)	549 ± 52	0.991	586 ± 73	0.994	7
Subcutaneous fat	343 ± 37	0.997	382 ± 13	0.999	11
Uterus					
Myometrium	1,309 ± 35	0.998	1,514 ± 156	0.999	16
Endometrium	1,274 ± 64	0.997	1,453 ± 123	0.998	14
Cervix	1,135 ± 154	0.998	1,616 ± 61	0.998	42
Prostate	1,317 ± 85	0.999	1,597 ± 42	0.998	21

* Data are mean ± SD.
† Difference is significant ($P < .05$).

TABLE 2
Average T2 Relaxation Times at 1.5 and 3.0 T

Tissue	1.5 T		3.0 T		
	T2 Relaxation Time (msec)*	R^2 Value (%)	T2 Relaxation Time (msec)*	R^2 Value (%)	Difference (%)
Kidney					
Cortex	87 ± 4	0.993	76 ± 7	0.993	−13†
Medulla	85 ± 11	0.992	81 ± 8	0.996	−5
Liver	46 ± 6	0.992	34 ± 4	0.984	−26†
Spleen	79 ± 15	0.998	61 ± 9	0.996	−23†
Pancreas	46 ± 6	0.989	43 ± 7	0.977	−7
Paravertebral muscle	27 ± 8	0.925	29 ± 4	0.867	7
Bone marrow (L4 vertebra)	49 ± 8	0.997	49 ± 4	0.994	1
Subcutaneous fat	58 ± 4	0.995	68 ± 4	0.999	17†
Uterus					
Myometrium	117 ± 14	0.995	79 ± 10	0.993	−33
Endometrium	101 ± 21	0.987	59 ± 1	0.999	−42
Cervix	58 ± 20	0.993	83 ± 7	0.992	43
Prostate	88 ± 0	0.997	74 ± 9	0.995	−16

* Data are mean ± SD.
† Difference is significant.

els ± 0) outside the body to quantify noise. This ROI was located to the right of the body on the transverse section and anterior to the body on the sagittal section. Artifactual signal, due either to motion or to single-shot fast SE related blurring, was avoided for noise measurement. The mean and SD of the signal in the empty region were recorded.

MR images were of similar quality in all subjects (Fig 1), and contrast-to-noise ratio and resolution were sufficient to define ROIs for all the tissues of interest. Motion between the acquisition of images with different TI and TE values was not an important problem in any of the subjects. In the phantoms, the ROI size was 36 pixels.

For our quantitative analysis, it was necessary to include noise in the images as a systematic factor, rather than just as a source of random variation. On MR images, the phase of the actual signal generated from each voxel is not known because hardware factors, imaging imperfections, and potential propagation of radiofrequency waves in the body alter the phase of the signal. Typically, this complexity is avoided by taking the magnitude, or absolute value, of the signal intensity. In magnitude images with low signal-to-noise ratio, noise adds a constant term to the measured intensity. The exact mathematical form of this constant has been derived for an arbitrary number of receiver coils in terms of confluent hypergeometric functions (7), but use of this expression would greatly complicate the analysis. Instead, we observed that the true expression was well approximated by the simple function

$$SI = \sqrt{S^2 + C_n^2}, \quad (1)$$

where SI is the measured signal intensity when averaged over time or an ROI, S is the true signal intensity (in the absence of noise) from tissue, and C_n is a noise-related constant. The exact and approximate expressions are compared in Figure 3. While the relationship between C_n and the noise level depends on the number of coils and the degree of correlation between the noise in the coils, C_n itself can be measured simply as the mean of the signal intensity in a region devoid of true signal intensity.

T1 and T2 relaxation times for imaging data were obtained by fitting the MR signal intensity of a selected ROI in each image. All curve fitting was performed with Kaleidagraph software (Abelbeck Software, Reading, Pa). Estimates of T1 and T2 relaxation times were obtained from the nonlinear least square fit of the signal intensity measured for each TI and TE value, respectively, by using the corresponding measured noise. Iterations

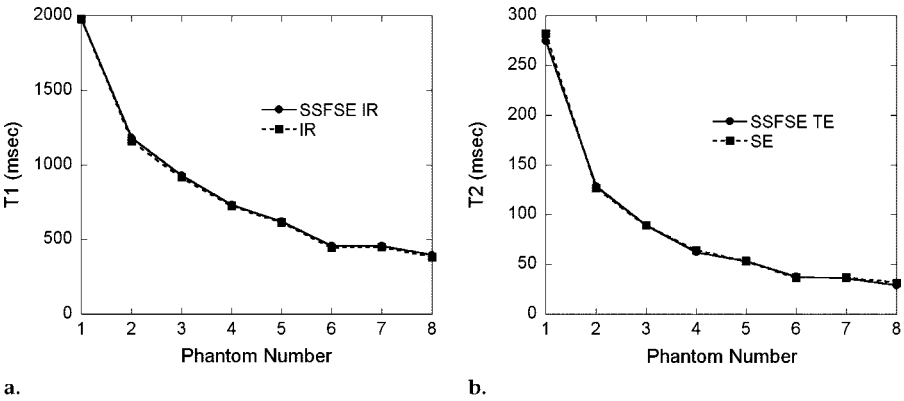

a. b.

Figure 4. **(a)** T1 relaxation times in phantoms obtained with the single-shot fast SE sequence (solid line) and the standard inversion-recovery method (dashed line). We used eight phantoms with different concentrations of $MnCl_2$ in water. The mean relative difference in T1 relaxation time for each phantom was less than 2%, with an SD between differences of 1%. **(b)** T2 relaxation times in the same phantoms obtained with the single-shot fast SE sequence (solid line) and the standard SE method (dashed line). The mean relative difference in T2 relaxation time for each phantom was found to be 3%, with an SD between differences of 3%.

were performed until the χ^2 value changed by less than 1% starting from an initial relaxation time of 1,000 msec for T1 and 100 msec for T2.

On the inversion-recovery images, the signal intensity (8) follows Equation (2):

$$SI = \sqrt{(S_0 - 2 \cdot S_0 \cdot \exp^{-(TI/T1)} + S_0 \cdot \exp^{-(T_{sat}/T1)})^2 + C_n^2}, \quad (2)$$

where C_n is the noise-related constant of Equation (1). T_{sat} is the saturation time (4,500 msec) and is not equal to TR, because the refocusing pulses of the single-shot fast SE sequence continue to saturate the signal for their 500 msec duration. S_0 is a calibration constant that includes the water density, the sensitivity of the coils, and the gain of the MR imager. By using the square of the signal in Equation (1), the sign confusion that can occur with inversion-recovery imaging and magnitude images is avoided.

For the SE prepared images, the signal intensity follows a monoexponential decay, as shown in Equation (3):

$$SI = \sqrt{(S_0 \cdot \exp^{-(TE/T2)})^2 + C_n^2}. \quad (3)$$

Statistical Analysis

Phantoms.—For all phantoms, the relative differences in measured T1 relaxation time between the prepared single-shot fast SE sequence and the multiexcitation inversion-recovery technique and the relative differences in measured T2 relaxation time between the prepared single-shot fast SE sequence and the multiexcitation SE technique were calculated by using Equation (4):

$$RD = \frac{RT_{ref} - RT_{SSFSE}}{RT_{ref}}, \quad (4)$$

where RT_{ref} is the reference relaxation time and is the relaxation time measured with the multiexcitation inversion-recovery technique or the multiexcitation SE technique, and RT_{SSFSE} is the single-shot fast SE relaxation time, which is the relaxation time measured with the prepared single-shot fast SE sequence. The relative differences (represented as RD) were averaged, and the SD was calculated.

Volunteers.—T1 and T2 relaxation times at 1.5 and 3.0 T were averaged across subjects for all organs.

The SD between volunteers and the average of the correlation coefficients (R^2) of the fits were also calculated as measures of uncertainty.

The mean T1 relaxation times of the kidney cortex and medulla, liver, paravertebral muscle, spleen, bone marrow, and subcutaneous fat at 1.5 T were compared with relaxation times at 1.5 T in other studies (3,4) by means of a two-sample two-tailed *t* test. For T2 relaxation times, however, Bottomley et al (3) did not report sample size or SD. Thus, the two-sample two-tailed *t* test was performed with the assumption that the reported data had a lower SD and/or a higher number of patients, such that the mean was highly accurate. This assumption resulted in an overly strict comparison but permitted a qualitative estimate of the agreement between the literature and the experimental measurements in this study. Differences in mean relaxation times between 1.5 T (represented as $RT_{1.5}$) and 3.0 T (represented as $RT_{3.0}$) in each of the tissues were also analyzed with a two-sample two-tailed paired *t* test. In Tables 1 and 2, the differences are expressed in percent:

$$\text{Difference} = \frac{RT_{3.0} - RT_{1.5}}{RT_{1.5}}. \quad (5)$$

RESULTS

Validation

The accuracy of the prepared single-shot fast SE sequence for measuring T1 and T2 relaxation times was confirmed when compared with the multiexcitation inversion-recovery and SE sequences at 3.0 T. Because of the longer image acquisition time, the signal-to-noise ratio of the multiexcitation inversion-recovery and SE sequences was approximately four times greater than that of the corresponding single-shot fast SE images. The mean relative difference in measured T1 relaxation time between the prepared single-shot fast SE sequence and the multiexcitation inversion-recovery technique was 2% with an SD of 1%, as shown in Figure 4a. For T2 relaxation time, the mean relative difference between the prepared single-shot fast SE sequence and the multiexcitation SE technique was 3% with an SD of 3%, as shown in Figure 4b.

Volunteers

Two representative examples of 3.0-T single-shot fast SE transverse sections obtained with six different TI and TE values for the measurement of T1 and T2 relaxation times are shown in Figures 5a and 6a, respectively. Because magnitude images were reconstructed, the signal intensity of tissues such as fat that have a shorter T1 relaxation time exhibits a complicated intensity variation with TI. Signal intensity is high for short TI, when the true signal is negative, passes through a point of null signal intensity at intermediate TI, and then regains signal intensity at long TI when the signal is positive. The signal intensity curves obtained from different tissues fit well to the models of Equations (2) and (3). The T1 and T2 relaxation time curves and fits in liver, the kidney cortex and medulla, pancreas, and subcutaneous fat—which were measured by using MR images (Figs 5a, 6a)—are shown in Figures 5b and 6b.

Quantitative T1 and T2 relaxation times obtained from the fits were consistent across subjects with an SD of less

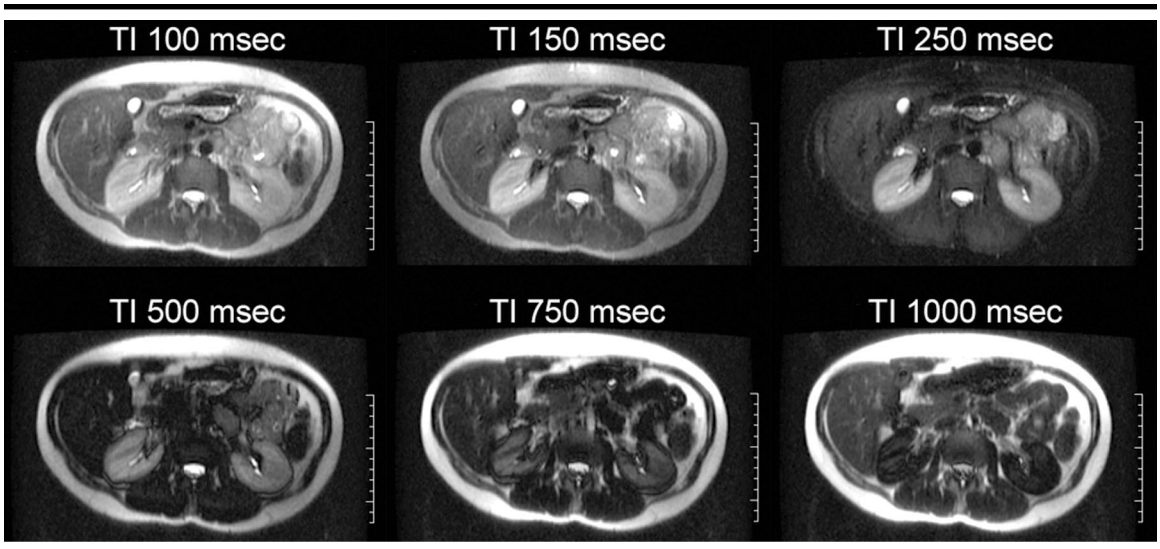

a.

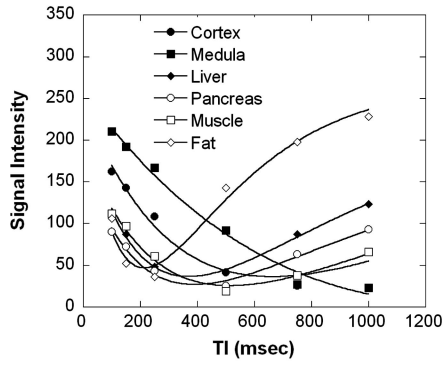

b.

Figure 5. **(a)** Transverse MR images obtained through the level of the kidney at 3.0 T with a half-Fourier acquisition single-shot fast SE sequence combined with inversion recovery (field of view, 360 × 252; section thickness, 5 mm; acquisition matrix, 256 × 160; effective TE, 60). Six TIs (100, 150, 250, 500, 750, and 1,000 msec) were used to measure T1 relaxation time, with a constant TR of 5,000 msec. The imaging reconstruction produced magnitude images, so large positive and negative values appear as areas of high signal intensity. The scale is in centimeters. **(b)** Graph shows signal intensities in the ROIs as a function of inversion-recovery TI time, as measured in the images shown in **a.** Fitted curves are shown as continuous lines through the data points and were used to measure T1 relaxation time.

than 10% of the mean relaxation time in most tissues. Smaller tissues with greater potential for partial volume errors and motion between images generally had higher SDs. Tables 1 and 2 summarize the T1 and T2 relaxation times, respectively, at 1.5 and 3.0 T in each of the studied tissues, which are shown in Figure 1. Mean R^2 values between volunteers were found to be 0.996 and 0.993 for T1 relaxation time and 0.996 and 0.995 for T2 relaxation time at 1.5 and 3.0 T, respectively. The mean noise level was 23.8 ± 2.58 for T1 relaxation time and 23.06 ± 1.6 for T2 relaxation time. This noise level was five to 10 times less than the peak signal intensity of the relaxation curves.

The accuracy of this technique was shown at 1.5 T by comparing the results of our study with results found in other studies (3,4). No significant differences in T1 relaxation time were found between our results and those reported in the literature for the liver, kidney cortex and medulla, spleen, and paravertebral muscle ($P > .05$), as shown in Table 3; however, a significant difference was found for adipose, in subcutaneous fat, and in bone marrow ($P < .007$). The reference T2 relaxation times correspond to relaxation times obtained for the kidney cortex in rats, for the liver in humans, for muscle in rats and mice, and for fat at 20°C in humans. For all tissues, a significant difference ($P < .06$) was found, which could be due to the temperature, the in vivo versus in vitro conditions, and species dependences of tissue T2 relaxation times (3).

The comparison at 1.5 and 3.0 T showed a mean increase of 19% for T1 relaxation time and a mean decrease of 8% for T2 relaxation time at higher magnetic strength. The difference for T1 relaxation times was significant ($P < .05$) for the kidney cortex, liver, and spleen. Significant differences in T2 relaxation times between 1.5 and 3.0 T were found in the kidney cortex, spleen, pancreas, and subcutaneous fat ($P < .05$).

DISCUSSION

The resulting mean T1 relaxation times at 1.5 T for the kidney, liver, spleen, and paravertebral muscle are in good agreement with the data reported in the literature (3,4); however, the T1 relaxation time in the subcutaneous fat was higher in our study (344 msec) than that reported in the literature (200 msec). While the T1 relaxation time of fat is shorter than that of any other tissue studied, we were unable to identify a potential experimental error responsible for the lengthened T1 relaxation time we observed. It has been demonstrated that adipose tissue has multiple components with different T1 and T2 relaxation times and different frequency components (9). Differences in imaging methods and T2 relaxation time measurement, combined with the complex relaxation characteristics of adipose tissue, may be responsible for the differences in measured relaxation times.

For measurement of T1 relaxation time, the TR was 5,000 msec. This TR value was five times greater than the mean measured T1 relaxation time, which is required to measure the T1 value accurately (6). For measurement of T2 re-

TABLE 3
Comparison of T1 and T2 Relaxation Times Measured at 1.5 T

Tissue	Present Study		Bluml et al 1993 (4)			Present Study		Bottomley et al 1984 (3)	
	T1 Relaxation Time (msec)*	No. of Patients	T1 Relaxation Time (msec)*	No. of Patients	*P* Value	T2 Relaxation Time (msec)*	No. of Patients	T2 Relaxation Time (msec)*	*P* Value
Kidney									
Cortex	966 ± 58	4	966 ± 41	6	.998	87 ± 4	4	56	<.001
Medulla	1,412 ± 58	4	1,320 ± 76	3	.187				
Liver	586 ± 39	4	570 ± 43	11	.553	46 ± 6	4	35	.047
Spleen	1,057 ± 42	4	1,026 ± 62	4	.507				
Paravertebral muscle	856 ± 61	4	891 ± 42	6	.359	27 ± 8	4	60	.005
Bone marrow (L4 vertebra)	549 ± 52	4	1,013 ± 106	6	<.001				
Fat	343 ± 37	4	200 ± NA†	NA†	.007	58 ± 4	4	52	.059

* Data are mean ± SD.
† NA = not applicable.

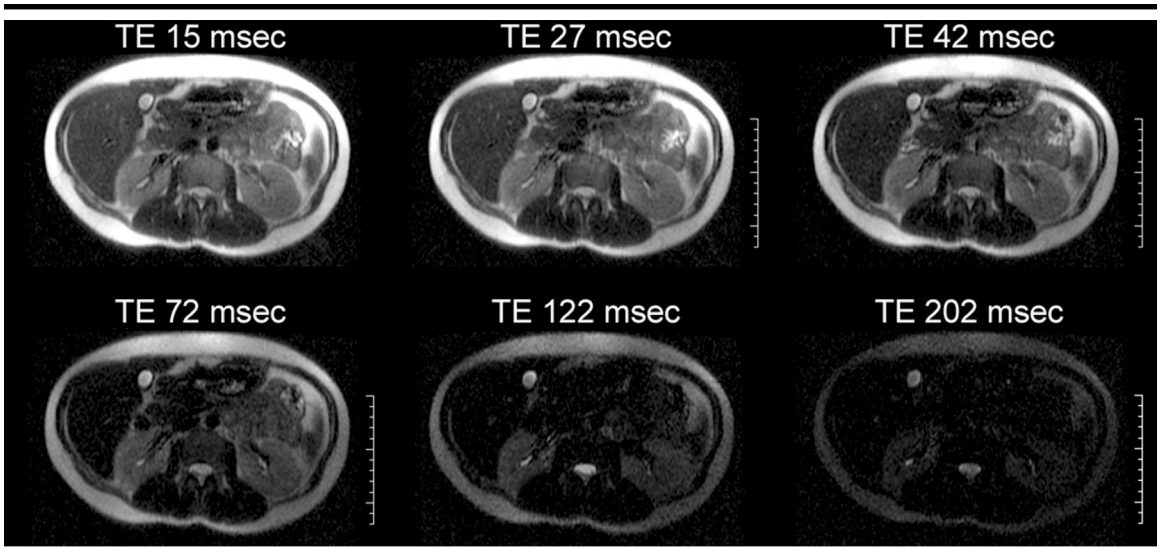

a.

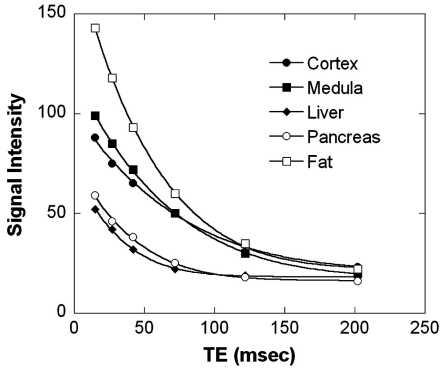

b.

Figure 6. **(a)** Transverse MR images obtained through the level of the kidney at 3.0 T with a half-Fourier acquisition single-shot fast SE sequence combined with SE preparation (field of view, 360 × 252; section thickness, 5 mm; acquisition matrix, 256 × 160; effective TE, 60 msec). Six preparation TEs (15, 27, 42, 72, 122, and 202 msec) were used to measure the T2 relaxation time with a constant TR of 2,000 msec. With a short T2 relaxation time (37 msec), the signal decayed more rapidly in the liver than in fat, which exhibited a longer T2 relaxation time (66 msec). The scale is in centimeters. **(b)** Signal intensities in the ROIs as a function of SE preparation time and TI, as measured in the images in **a.** Fitted curves are shown as continuous lines through the data points and were used to measure T2 relaxation time.

laxation time, the TRs of 2 seconds for the single-shot fast SE sequence and 3 seconds for the multiexcitation SE sequence used for validation were selected as a compromise between speed of acquisition and T1 recovery of magnetization. Since simple fluids have a T1 relaxation time that is longer than these TRs and a T2 relaxation time that is comparable with these TRs, systematic errors from stimulated echoes and other imperfections would be likely to corrupt the measurement of T2 relaxation time in such fluids. Only soft tissues were evaluated with this sequence. T2 relaxation time can be shortened by the diffusion of water around magnetic molecules, such as hemoglobin in deoxygenated blood. Such effects increase with the field strength and the magnetic properties of iron in the liver (10) may be partially responsible for the larger shortening of

T2 relaxation time in the liver we observed at 3.0 T. T2 contrast in standard fast SE sequences differs because multiple refocusing pulses attenuate the effect of the diffusion related phenomenon on image intensity.

Normal biologic variations can explain the higher subject-to-subject variability found for T1 relaxation time in bone marrow and the kidney cortex. Indeed, the fraction of fat in the bone marrow can vary physiologically, which changes the relaxation times dramatically (11). Imperfect separation of cortex and medulla in the kidney may have contributed to the higher error in these regions.

At 3.0 T, it is difficult to compare our results with those reported in the literature, because—to our knowledge—no study of relaxation times of the body, in vivo, has been performed. It is well established that the relaxation time in tissue depends on the magnetic field, temperature, time after excision, and in vivo or in vitro conditions (3).

The different fractional changes in T1 and T2 relaxation times of different tissues suggest that image contrast may either increase or decrease with field strength depending on the tissues that are being studied. The measurements reported here may help to guide the selection of those body applications that are most likely to benefit from 3.0-T MR imaging.

References

1. Duewell S, Wolff SD, Wen H, Balaban RS, Jezzard P. MR imaging contrast in human brain tissue: assessment and optimization at 4 T. Radiology 1996; 199:780–786.
2. Wansapura JP, Holland SK, Dunn RS, Ball WS Jr. NMR relaxation times in the human brain at 3.0 Tesla. J Magn Reson Imaging 1999; 9:531–538.
3. Bottomley PA, Foster TH, Argersinger RE, Pfeifer LM. A review of normal tissue hydrogen NMR relaxation times and relaxation mechanisms from 1–100 MHz: dependence on tissue type, NMR frequency, temperature, species, excision, and age. Med Phys 1984; 11:425–448.
4. Bluml S, Schad LR, Stepanow B, Lorenz WJ. Spin-lattice relaxation time measurement by means of a TurboFLASH technique. Magn Reson Med 1993; 30:289–295.
5. Fautz HP, Buchert M, Husstedt H, Laubenberger J, Hennig J. TSE-sequences with spin-echo contrast. Magn Reson Med 2000; 43:577–582.
6. Jezzard P, Duewell S, Balaban RS. MR relaxation times in human brain: measurement at 4 T. Radiology 1996; 199:773–779.
7. Constantinides CD, Atalar E, McVeigh ER. Signal-to-noise measurements in magnitude images from NMR phased arrays. Magn Reson Med 1997; 38:852–857.
8. Young IR, Bydder GM. Contrast development and manipulation in MR imaging. In: Atlas SW, ed. Magnetic resonance imaging of the brain and spine. Vol 1. 3rd ed. Philadelphia, Pa: Lippincott Williams & Wilkins, 2002; 47.
9. Graham SJ, Ness S, Hamilton BS, Bronskill MJ. Magnetic resonance properties of ex vivo breast tissue at 1.5 T. Magn Reson Med 1997; 38:669–677.
10. Kreeftenberg HG Jr, Mooyaart EL, Huizenga JR, Sluiter WJ. Quantification of liver iron concentration with magnetic resonance imaging by combining T1-, T2-weighted SE sequences and a gradient echo sequence. Neth J Med 2000; 56:133–137.
11. Hajek PC, Baker LL, Goobar JE, et al. Focal fat deposition in transverse bone marrow: MR characteristics. Radiology 1987; 162: 245–249.